PERIODIC UNIT-CELL SIMULATION FOR TRANSVERSE TENSILE FAILURE OF UNIDIRECTIONAL COMPOSITES WITH COHESIVE ZONE MODEL

J. Koyanagi[1*], Y. Sato[2], T. Okabe[2], S. Yoneyama[3]

[1]*Institute of Space and Astronautical Science, Japan Aerospace Exploration Agency, 3-1-1 Yoshinodai, Chuo-ku Sagamihara, Kanagawa Japan*
[2]*Department of Aerospace Engineering, Tohoku University, 6-6-01, Aoba-yama, Aoba-ku, Sendai, Miyagi Japan*
[3]*Department of Mechanical Engineering, Aoyama Gakuin University, 5-10-1 Fuchinobe, Chuo-ku Sagamihara, Kanagawa, Japan*
**koyanagi.jun@jaxa.jp*

Keywords: Periodic Unit-Cell Simulation, Polymer Matrix Composite, Transverse Failure, Cohesive Zone Model, Strain-Rate Dependence

Abstract
This study investigates strain-rate dependent transverse tensile failure of unidirectional composite materials with a periodic unit-cell simulation. The unit cell consists of 20 fibers aligned at random in the matrix. Elasto-viscoplastic constitutive equation including continuum damage mechanics is used for the matrix. This enables us to simulate strain-rate dependence of matrix plastic deformation and damage. For the fiber/matrix interface, cohesive zone model is also employed. Interface failure under combined stress state of normal and shear is considered. Fibers are assumed to be elastic body. When strain rate is relatively high, naturally, the maximum matrix stress is relatively large due to the viscoplastic properties so that the interface tends to fail in advance of matrix yielding and/or failure. On the contrary, when strain rate is low, the maximum matrix stress becomes small and interface failure does not appear.

1 Introduction

Polymer composite materials have been used widely, especially in a aerospace fields because of well-known high specific strength and modulus. A transverse crack is what we call first-ply-failure, sometimes becomes considerable damage in terms of leak problem, and can be trigger of fatal delamination damage. A precise estimation of transverse cracking initiation is necessary for further reliability of composite utilizations. In order to predict the transverse cracking initiation, it is simply inevitable to understand the characteristics of transverse failure of unidirectional composites. In our previous work [1, 2], the transverse failure of unidirectional composites is studied. It was experimentally found that the failure mode transit with strain rate as shown in Fig. 1. When the strain rate is high, the composite fails in interface failure dominant mode. When the strain rate is low, it fails in matrix failure dominant mode. The paper concludes that the time dependence of interface strength is much less than that of matrix strength.

(a) High-strain rate (b) Intermediate-strain rate (c) Low-strain rate

Fig. 1 Transverse failure surface examined by various strain rates

In this study, the characteristic of transverse failure in unidirectional composite dominated by strain rate is numerically simulated. We implement periodic unit-cell simulation. The unit cell consists of 20 fibers and surrounding matrix. For the fiber elastic body is assumed. An elasto-viscoplastic constitutive equation based on damage mechanics is applied to the matrix. A cohesive zone model is employed for the fiber/matrix interface. Comparing the simulation results with experimental results in terms of failure mode, specimen strength and stress-strain curves, the parameters used in elasto-viscoplastic constitutive equation and cohesive element are estimated.

2 Analytical procedure

2.1 Periodic unit-cell simulation

This study employs 2D-unit cell as shown in Fig. 2. The unit cell consists of 20 fibers and matrix. The fiber array is at random. The unit cell is divided into 100,000 of elements, approximately. Fiber diameter is 3.5μm, and the fiber volume fraction is 55%. Periodic boundary conditions are applied to the corresponding edges in the unit cell.

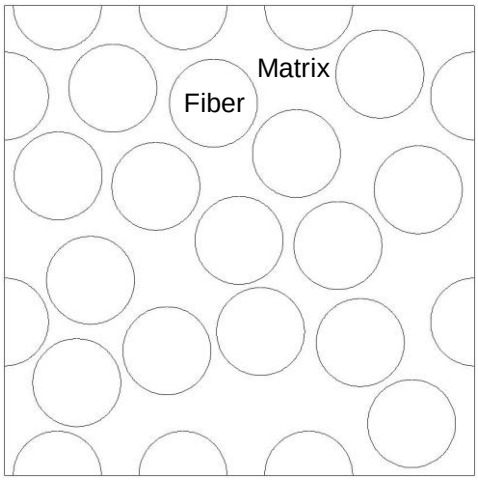

Fig. 2 Unit cell for numerical simulation, including 20 fibers

2.2 Modeling for matrix

Stress-strain response of thermoplastic resin is modeled by one parameter damage modeling equations suggested by Kobayashi et al [3], in which the constitutive equation including the effect of damage is defined by following equations.

$$\dot{\boldsymbol{\sigma}} = (1-D)\mathbf{C}^{v} : \dot{\boldsymbol{\varepsilon}} - (1-D)\frac{3\mu\dot{\bar{\varepsilon}}^{p}\cos\delta}{\bar{\sigma}}\boldsymbol{\sigma}' - \frac{\dot{D}}{1-D}\boldsymbol{\sigma} \qquad (1)$$

$$\mathbf{C}^v = \frac{H}{H+3\mu}\left[\mathbf{C}^e + \frac{3\mu}{H}\left\{\frac{3\lambda+2\mu}{3}\mathbf{I}\otimes\mathbf{I} + 3\mu\frac{\boldsymbol{\sigma}'\otimes\boldsymbol{\sigma}'}{\bar{\sigma}^2}\right\}\right]$$

$$H = \frac{1}{1-D}\frac{\dot{\bar{\sigma}}}{\dot{\bar{\varepsilon}}^p k},\ \bar{\sigma} = \sqrt{\frac{3}{2}\boldsymbol{\sigma}':\boldsymbol{\sigma}'},\ \dot{\bar{\sigma}} = \sqrt{\frac{3}{2}\dot{\boldsymbol{\sigma}}':\dot{\boldsymbol{\sigma}}'}$$

where δ is non-coaxial angle, k is non-coaxial parameter, λ is Lame's constant. $\dot{\bar{\varepsilon}}^p$ is expressed as following equation employing a hardening law for a ductile polymer material.

$$\dot{\bar{\varepsilon}}^p = \dot{\varepsilon}_r\left(\frac{\bar{\sigma}}{g(\bar{\varepsilon}^p)}\right)^{\frac{1}{m}} \qquad \dot{\bar{\varepsilon}}^p = \dot{\varepsilon}_r\left(\frac{\bar{\sigma}+\beta\sigma_m}{g(\bar{\varepsilon}^p)}\right)^{\frac{1}{m}} \tag{2}$$

$$g(\bar{\varepsilon}^p) = \sigma_r\left\{\tanh(k_1\bar{\varepsilon}^p) + k_2 + H_e(\bar{\varepsilon}^p - \varepsilon_r)k_3(\exp\bar{\varepsilon}^p - \exp\varepsilon_r)\right\}$$

where m is strain rate sensitivity exponent, $\dot{\varepsilon}_r$ is reference strain rate, ε_r is reference strain, σ_r is initial yield stress, and k_1, k_2, k_3 are material constants. Non-coaxial angle between $\boldsymbol{\sigma}'$ and $\boldsymbol{\varepsilon}^p$, is δ given by

$$\sin\delta = k\sin\alpha\ . \tag{3}$$

$$\text{where}\quad k = \begin{cases} p_1\sin\left(\dfrac{\pi}{2}\dfrac{m}{p_2}\right) & (0 \le m \le p_2) \\ p_1\left\{\tanh\left[-p_3(m-p_2)\right]+1\right\} & (p_2 \le m) \end{cases}\ .$$

Here, p_1, p_2, p_3 are material constants. α is angle between $\boldsymbol{\sigma}'$ and $\dot{\sigma}'$, defined by

$$\cos\alpha = \frac{\dot{\bar{\sigma}}}{\dot{\bar{\sigma}}}\ . \tag{4}$$

Damage parameter D inducing stiffness decrease is given by [4]

$$\dot{D} = \frac{\bar{\sigma}^2}{2EC(1-D)^2}\left\{\frac{2}{3}(1+\nu)+3(1-2\nu)\left(\frac{\sigma_m}{\bar{\sigma}}\right)^2\right\}\dot{\bar{\varepsilon}}^p \tag{5}$$

$$\dot{\varepsilon}_m^p = \left\{(q_1 D)\cosh(q_2\,\sigma_m/\sigma_r)\right\}^{\bullet} \tag{6}$$

where E is Young's modulus of matrix and C is material constant. When the value of D in each element reaches 0.25, the element is recognized as completely damaged and is then removed. In order to eliminate a mesh dependence issue for matrix damage, non-localization yielding the following equation for D at position x is applied. [5, 6]

$$D(\boldsymbol{x}) = \frac{1}{V_r(\boldsymbol{x})}\int_V h(\boldsymbol{s}-\boldsymbol{x})D_{\text{elem}}(\boldsymbol{s})dV(\boldsymbol{s}) \tag{7}$$

Here, $D_{\text{elem}}(\boldsymbol{s})$ is damage of element at position s and V is reference volume. $h(\boldsymbol{x})$ and V_r are given by

$$h(\boldsymbol{x}) = \exp\left\{-\frac{n|\boldsymbol{x}|^2}{l^2}\right\} \tag{8}$$

$$V_r(\boldsymbol{x}) = \int_V h(\boldsymbol{s}-\boldsymbol{x})dV(\boldsymbol{s}) \tag{9}$$

Here, n is number of dimension. $n = 2$ is used in this study. l is reference length regarding the non-localization. $l = 0.15$ μm is used in this study. In the present study, $D^*(D)$ defined by following equation is employed instead of D in Eq. (1), for the expression of rapid damage progress [5].

$$D^* = \begin{cases} D & (D < D_c) \\ D_c + \dfrac{D_f^* - D_c}{D_f - D_c}\left(D - D_f\right) & (D \geq D_c) \end{cases} \tag{10}$$

$$\dot{D}^* = \begin{cases} \dot{D} & (D < D_c) \\ \dfrac{D_f^* - D_c}{D_f - D_c}\dot{D} & (D \geq D_c) \end{cases} \tag{11}$$

D_c is specific damage value. When D is greater than D_c, the rapid damage progress is considered. D^*_f means element failure. This study assumes $D_c = 0.08$, $D_f = 0.25$ and $D_f^* = 1/1.5$ [5].

2.3 Modeling for fiber/matrix interface

This study inserts cohesive element into the fiber/matrix interface. In terms of convergence property in numerical analysis, Dugdale-type cohesive element is used in this study. The traction separation relationship of the cohesive element is shown in Fig. 3. In the present study, normal mode of interface failure is considered. Time dependence of the interface property is neglected [1, 2].

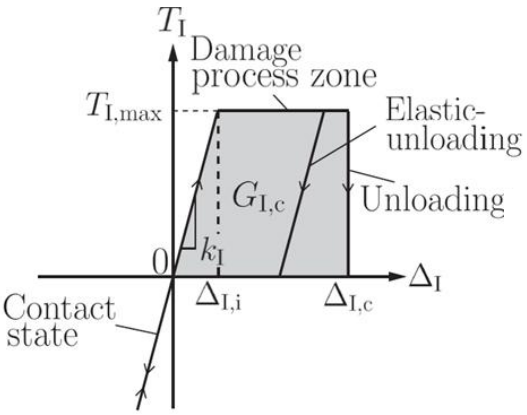

Fig. 3 Traction-separation behavior of cohesive element

3 Analytical results

Stress-strain curves obtained from the analysis assuming 70MPa of interface normal strength and 2.0N/m of interface fracture energy are shown in Fig. 4. Both ultimate stress and strain decrease with decrease of strain-rate. This result is qualitatively consistent with experimental result [1, 2].

Failure mode difference due to the strain-rate difference is depicted in Fig. 5. The left-hand side figures show damage distributions and right figures highlight failure cohesive element. As shown in the figures, the low-strain rate derives matrix failure dominant mode and high-strain rate leads to interface failure dominant mode, which are consistent with experimental results. It can be identified that Fig. 5 (a) and Fig.1 (a) are similar and Fig. 5 (b) and Fig. 1 (c) are also similar in respect to the failure mode. Thus, introducing the elasto-viscoplastic characteristic and cohesive element into matrix and interface, respectively, the failure mode transition due to the strain rate difference is successfully followed by the periodic unit-cell simulation.

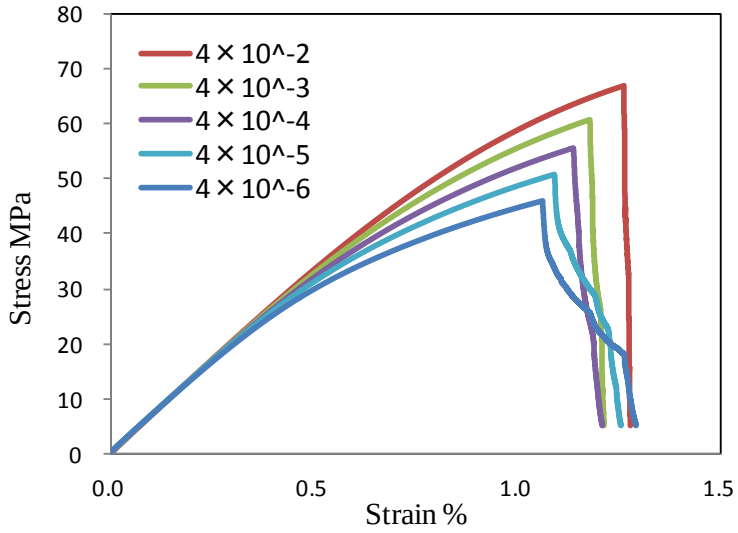

Fig. 4 Stress-strain curves obtained from analysis assuming 70MPa of strength and 2.0N/m of fracture energy for inserted cohesive element

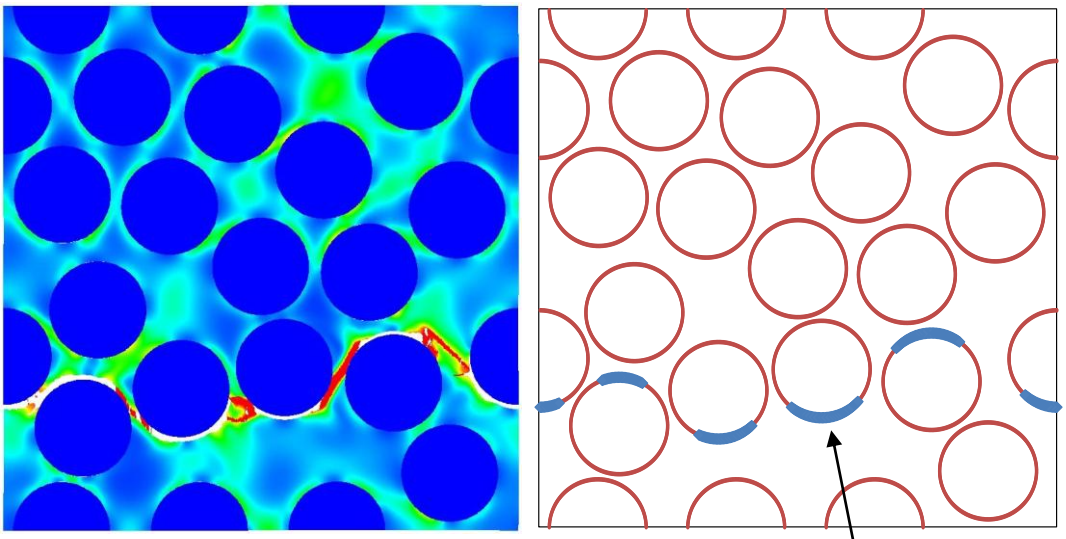

(a) High strain rate (4.0 x 10^{-2}): Interface failure dominant mode

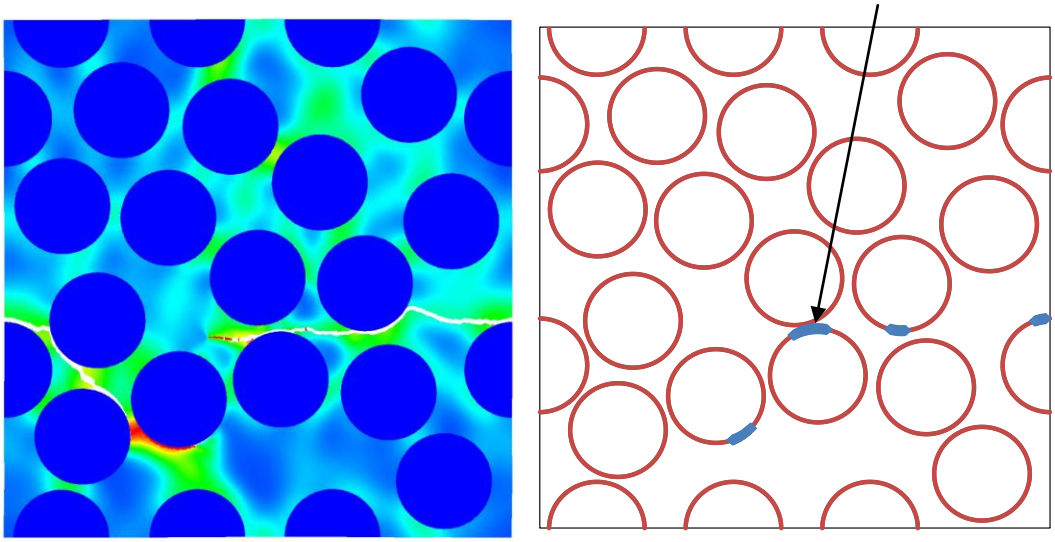

(b) Low strain rate(4.0 x 10^{-6}): Matrix failure dominant mode

Fig. 5 Damage distributions of matrix element (left) and interface element (right)

Relationships between bonding length normalized by the unit-cell length and strain rate when assuming several set of properties for the cohesive elements are shown in Fig. 6. If relatively high fracture energy is assumed, the interfaces tend not to fail independently on strain rate. This means that the failure mode transition does not appear. Experiments actually show interface failure dominant mode so that it is implied that the fracture energy of interface should be relatively low. The value of 2.0 J/m for the fracture energy is much less than that of CFRP itself. This is interesting aspect to be studied as our subsequent study.

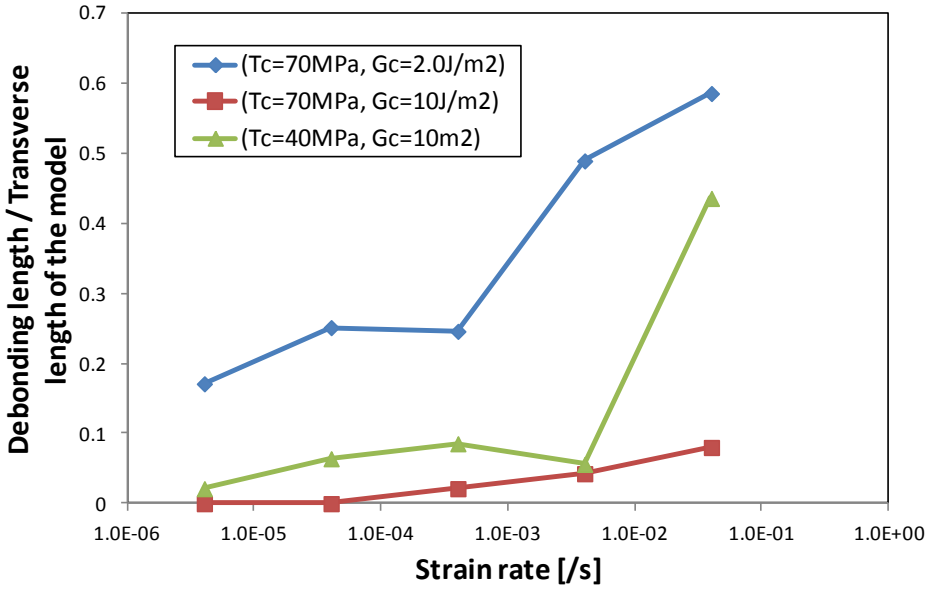

Fig. 6 Relationship between debonding length normalized by unit-cell length and strain rate

3 Conclusion

The present study numerically simulates time dependence of transverse tensile failure for unidirectional CFRP. At high-strain rate, interface failure dominant mode appears and, on the contrary, matrix failure dominant mode is indicated at low-strain rate. The analytical results are basically consistent with experimental observation. However, when the fracture energy of the interface is relatively high, the strain-rate governing failure-mode transition does not occur. For the occurrence of failure mode transition, the fracture energy of interface is implied to be less than specific value.

References

[1] Koyanagi J, Yoneyama S, Eri K, PD Shah, Time dependency of carbon/epoxy interface strength, *Composite Structures* **92**, 150-154 (2010).
[2] Koyanagi J, Yoneyama S, Nemoto A, Melo J, Time and temperature dependence of carbon/epoxy interface strength, *Composites Science and Technology* **70**, 1395-1400 (2010)
[3] Kobayashi, S., Tomii, D., Shizawa, K., A Modelling and Simulation on Failure Prediction of Ductile Polymer Based on Craze Evolution and Annihilation, *Transactions of the Japan Society of Mechanical Engineers, Series A* **70**, 810-817 (2004).
[4] Lemaitre J, How to use damage mechanics, *Nuclear Engineering and Design* **80**, 233-245 (1984)
[5] Tvergaard V, Needleman A, Nonlocal effects on localization in a void-sheet, *International Journal of Solid Structures* **32**, 1063-1077 (1995)
[6] Pijaudier-Cabot G, Bazant ZP, Nonlocal damage theory, *Journal of Engineering Mechanics ASCE* **113,** 1512-1533(1987)